

# Antisense Glutaminase Inhibition Modifies the O-GlcNAc Pattern and Flux Through the Hexosamine Pathway in Breast Cancer Cells

Ana C. Donadio,<sup>1</sup> Carolina Lobo,<sup>2</sup> Marta Tosina,<sup>2</sup> Vanessa de la Rosa,<sup>2</sup> Mercedes Martín-Rufián,<sup>2</sup> José A. Campos-Sandoval,<sup>2</sup> José M. Matés,<sup>2</sup> Javier Márquez,<sup>2</sup> Francisco J. Alonso,<sup>2</sup> and Juan A. Segura<sup>2\*</sup>

<sup>1</sup>Departamento de Bioquímica Clínica, Centro de Investigaciones en Bioquímica Clínica e Inmunología, CIBICI-CONICET, Facultad de Ciencias Químicas, Universidad Nacional de Córdoba, Haya de la Torre y Medina Allende, Ciudad Universitaria, Córdoba CP5000, Argentina

<sup>2</sup>Departamento de Biología Molecular y Bioquímica, Facultad de Ciencias, Universidad de Málaga, 29071 Málaga, Spain

**Abstract** Glutamine behaves as a key nutrient for tumors and rapidly dividing cells. Glutaminase is the main glutamine-utilizing enzyme in these cells, and its activity correlates with glutamine consumption and growth rate. We have carried out the antisense L-type glutaminase inhibition in human MCF7 breast cancer cells, in order to study its effect on the hexosamine pathway and the pattern of protein O-glycosylation. The antisense mRNA glutaminase expressing cells, named ORF19, presented a 50% lower proliferation rate than parental cells, showing a more differentiated phenotype. ORF19 cells had an 80% reduction in glutamine:fructose-6-P amidotransferase activity, which is the rate-limiting step of the hexosamine pathway. Although the overall cellular protein O-glycosylation did not change, the O-glycosylation status of several key proteins was altered. O-glycosylation of O-GlcNAc transferase (OGT), the enzyme that links N-acetylglucosamine to proteins, was fivefold lower in ORF19 than in wild type cells. Inhibition of glutaminase also provoked a 10-fold increase in Sp1 expression, and a significant decrease in the ratio of O-glycosylated to total protein for both Sp1 and the Rpt2 proteasome component. These changes were accompanied by a higher Sp1 transcriptional activity. Proteome analysis of O-glycosylated proteins permitted the detection of two new OGT target proteins: the chaperonin TCP-1  $\theta$  and the oncogene Ets-related protein isoform 7. Taken together, our results support the hexosamine pathway and the O-glycosylation of proteins being a sensor mechanism of the nutritional and energetic states of the cell. *J. Cell. Biochem.* 103: 800–811, 2008. © 2007 Wiley-Liss, Inc.

**Key words:** O-GlcNAc transferase (OGT); Sp1; antisense mRNA; glutaminase; O-glycosylation

Glutamine is a major source of nitrogen and energy in rapidly dividing cells. Removing glutamine from culture medium promotes tumor cell differentiation and decreases pro-

liferation; inversely, addition of glutamine protects cells from apoptosis and induces proliferation [Medina et al., 1992; Tapiero et al., 2002; Matés et al., 2006]. Glutamine may behave as a cellular signal; for example, the early effects of glutamine on enterocytes are mediated by signaling through a MAPK cascade [Rhoads et al., 1997]. Glutamine signaling also involves other pathways such as mTOR [Nakajo et al., 2005] and MSK1 [Ko et al., 2001].

The main glutamine-metabolizing enzyme in rapidly dividing cells is glutaminase (EC 3.5.1.2, GA) although other enzymes, mainly amidotransferases, also make use of glutamine. Two major isoenzymes of GA have been described in mammals, namely liver (L)-type (LGA) and kidney (K)-type (KGA) isoforms which are encoded by different genes [Aledo

Ana C. Donadio and Carolina Lobo contributed equally to this work.

Grant sponsor: Ministry of Education and Science of Spain; Grant number: SAF 2004-02339; Grant sponsor: HUTESA, S.A.

\*Correspondence to: Juan A. Segura, Departamento de Biología Molecular y Bioquímica, Facultad de Ciencias, Universidad de Málaga, 29071 Málaga, Spain.

E-mail: jsegura@uma.es

Received 11 December 2006; Accepted 17 May 2007

DOI 10.1002/jcb.21449

© 2007 Wiley-Liss, Inc.

et al., 2000]. Recently, two GA isoforms have been cloned: a spliced variant of the K-type gene isolated from a human colon carcinoma and named GAC [Elgadi et al., 1999], and a human L-type GA cDNA cloned from ZR75 breast cancer cells [Gómez-Fabre et al., 2000]. Although previously thought to be expressed in mutually exclusive tissues, with KGA being amply distributed and LGA being restricted to adult liver [Smith and Watford, 1990; Curthoys and Watford, 1995], recent data have shown that both isozymes are simultaneously present in tissues and even co-expressed in the same cell types [Aledo et al., 2000; Turner and McGivan, 2003; Pérez-Gómez et al., 2005]. GA isozymes have been traditionally considered to be mitochondrial enzymes. However, a nuclear localization has been recently reported for LGA [Olalla et al., 2002], raising the possibility of an alternative function for this enzyme [Márquez et al., 2006]. GA is over-expressed in tumors and has been positively linked to tumor malignancy [Lobo et al., 2000]. Knocking down KGA expression by antisense technology in Ehrlich ascites tumor cells reduces proliferation, increases differentiation and makes the cells unable to grow in vivo due to the loss of their capacity to evade the host immune response [Lobo et al., 2000; Segura et al., 2001]. Glutamine:fructose-6-P amidotransferase (EC 2.6.1.16, GFAT) catalyzes the formation of glucosamine-6-P (GlcN-6-P) from fructose-6-P and glutamine, and represents the first and rate-limiting step in the de novo biosynthesis of hexosamines. The hexosamine pathway end product, UDP-N-acetylglucosamine (UDP-GlcNAc), is a precursor for the formation of all macromolecules containing amino sugars, including O-GlcNAc-modified proteins. O-glycosylation of nuclear and cytoplasmic proteins is a reversible modification that takes place in serine or threonine residues. Frequently the same O-glycosylated residues are also the target of serine/threonine kinases [Torres and Hart, 1984; Holt and Hart, 1986]. O-glycosylation reaction is catalyzed by the enzyme UDP-N-acetylglucosaminyl transferase (EC 2.4.1.94, O-GlcNAc transferase (OGT)). This enzyme has been shown to play a key role in signal transduction regulation, nuclear protein import and cytoskeletal organization [Wells et al., 2001]. Because O-GlcNAc levels in proteins appear to be sensitive to flux throughout the hexosamine pathway, the

availability of UDP-GlcNAc has been proposed as a general sensor of the nutritional state of the cell [Zachara and Hart, 2004].

The role of glutamine, a substrate of GFAT, in the modulation of the hexosamine pathway has been poorly characterized. GA inhibition causes a dramatic decrease of glutamine hydrolysis, and this may affect glutamine utilizing metabolic pathways. Our results show that GA inhibition greatly reduces GFAT activity and changes the O-GlcNAc pattern of key proteins that control cell proliferation and differentiation.

## MATERIALS AND METHODS

### Antibodies, Cell Lines, and Culture Conditions

Isoform specific anti-KGA and anti-LGA antibodies were obtained as described elsewhere [Pérez-Gómez et al., 2005]. The following antibodies were purchased:  $\beta$ -catenin (rabbit polyclonal, Abcam, UK), Rpt2 (rabbit polyclonal, Biomol), OGT (rabbit polyclonal, Sigma-Aldrich), Sp1 (clone 1C6, mouse monoclonal, Santa Cruz), TCP-1  $\theta$  (goat polyclonal, Santa Cruz), and O-linked GlcNAc (clone RL2, mouse monoclonal, Covance).

EATC, purchased from the American Tissue Culture Collection (ATCC), and its derivative 0.28AS-2 [Lobo et al., 2000] were grown in RPMI 1640 medium (Sigma) containing 2 mM glutamine and supplemented with 10% fetal bovine serum (FBS) and antibiotics. MCF7 cells, purchased from ATCC, and their derivative ORF19, were grown in DMEM medium (Sigma) supplemented with 10% FBS and antibiotics. Cultures were incubated in a humidified atmosphere at 37°C, with 5% CO<sub>2</sub>/95% air. The culture medium for cell lines containing the neomycin-resistance gene was supplemented with 600  $\mu$ g/ml G418.

### Construction of Plasmids Expressing Antisense-mRNA GA and Cell Transfections

The open reading frame of human L-type GA (GenBank # NM\_013267), in its antisense orientation, flanked by HindIII/EcoRI restriction sites was sub-cloned behind the CMV promoter of the pcDNA3 vector (Invitrogen, San Diego, CA). The construct was verified by restriction-enzyme digestion and sequencing of the DNA. The plasmid or the vector control pcDNA3 were transfected in MCF7 cells by lipofection using the lipid Dosper (Boehringer

Mannheim, Mannheim, Germany). Cells were selected after growing in DMEM medium containing 600  $\mu\text{g/ml}$  G418 for 2–3 weeks. Following G418 selection, 15 drug-resistant (neo+) clones were picked randomly from different plates and studied after expansion. As controls, six neo+ clones were picked from MCF7 cells transfected with the pcDNA3 vector lacking the antisense sequence (vector control cells). A colony-forming assay was performed by seeding the cells in triplicate with 250 cells/10-cm dish in complete medium. After 15 days of growth, the cells were fixed and stained with 5% Giemsa dye, and the grossly visible colonies were counted.

#### Measurement of Enzyme Activities

GA activity was assayed as described elsewhere [Heini et al., 1987] by measurement of the ammonia produced during the GA reaction after derivatization with *o*-phthaldialdehyde (OPA).

GFAT activity was determined as described previously [Daniels et al., 1996] with slight modifications. Exponentially growing cells were washed in PBS and scrapped with 0.7 ml of extraction buffer: 50 mM Hepes pH 7.5, 5 mM DTT and protease inhibitor cocktail (Complete Mini, Roche). After sonication, GFAT activity was assayed using once thawed cell extracts. Crude cell extract (11  $\mu\text{g}$ ) was incubated with 12 mM fructose-6-phosphate, 12 mM glutamine, 40 mM  $\text{NaH}_2\text{PO}_4$ , 1 mM EDTA, and 1 mM DTT (final vol. 100  $\mu\text{l}$ ), for 45 min at 37°C. The reaction was then stopped, and proteins were precipitated by the addition of 50  $\mu\text{l}$  1 M perchloric acid and incubated on ice for 10 min. After centrifugation at 16,000g for 10 min, 145  $\mu\text{l}$  of supernatant was extracted with 258  $\mu\text{l}$  of tri-*n*-octylamine:1,1,2-trichlorotrifluoroethane (1:4), and 120  $\mu\text{l}$  aqueous phase was then ready for HPLC analysis. The generated GlcN-6-P was detected by derivatization with 2 volumes OPA reagent (4 mg OPA in 50  $\mu\text{l}$  ethanol added to 5 ml 0.1 M sodium borate, pH 9.7, and 10  $\mu\text{l}$  2-mercaptoethanol) for 1 min, followed by neutralization with 120  $\mu\text{l}$  0.1 M sodium phosphate. After filtration through a 0.45  $\mu\text{m}$  filter, the sample was loaded onto a Spherisorb ODS-2 reverse phase column (25 cm  $\times$  4.6 mm, C18; Waters) and separated using a single gradient (0–6 min buffer A: 15 mM sodium phosphate, pH 7.2, 4.5% 2-propanol, 4.5% acetonitrile; 6–16 min gradient

to buffer B: 15 mM sodium phosphate, pH 7.2, 8% 2-propanol, 8% acetonitrile). Derivatized products were detected using a Beckman Coulter HPLC system (System Gold 126 Solvent Module).

#### GFAT Real-Time PCR

Total RNA was extracted from cultured cells using Tri-reagent (Sigma) and following manufacturer's directions. The purified RNA was dissolved in water and its quality was measured by the 260/280 absorbance ratio. RNA integrity was assessed by electrophoresis on 1% agarose gels. cDNA was synthesized from 1  $\mu\text{g}$  of total RNA using the Promega RT system according to the manufacturer's protocol.

Real-time PCR reactions were performed in a total volume of 25  $\mu\text{l}$  in the presence of 1 U of Taq DNA polymerase (Bio-Rad), 10  $\mu\text{l}$  SYBR Green (Sigma), 1 mmol/L dNTPs (Amersham), and 400 nM of forward and reverse PCR primers. Reactions were incubated in a MyiQ<sup>TM</sup> Real-Time PCR Detection System (Bio-Rad) under the following conditions: denaturation for 2.5 min at 95°C, and 35 cycles of 30 s at 94°C followed by 1 min at 58°C for mouse or 57°C for human cell lines. PCR primers for GFAT1, GFAT2 and mouse  $\beta$ -glucuronidase (GUS) were designed using the real-time PCR (TaqMan) online tool from Genescript, and primers for human GUS were obtained from the literature [Tzagarakis-Foster et al., 2002]. Primers are listed in Table I. To exclude the amplification of genomic DNA that might contaminate the samples, PCR primers were designed to cross exon junctions. The GUS gene was used as an internal control and RNA from the human neuroblastoma SH-SY5Y or mouse brain was used as a positive control for the GFAT2 gene in the PCR reactions. PCR products (10  $\mu\text{l}$ ) were analyzed on 1% agarose gels electrophoresed in 1 $\times$  TAE buffer (40 mM Tris-acetate, pH 8.5, 1 mM EDTA).

#### Isolation of Cellular Extracts

Culture medium was discarded, and the culture dishes were put on ice and washed three times with pre-cooled PBS. Whole cell extracts were obtained by lysing the cells on ice for 20 min in 350  $\mu\text{l}$  of lysis buffer (PBS, 1% (w/v) Nonidet P40, 0.5% (w/v) sodium deoxycolate, 0.1% (w/v) SDS plus protease inhibitor cocktail). The lysates were then sonicated for 20 s, spun at

TABLE I. Set of Primers Used for Real-Time PCR Experiments

Gen	Product size (pb)	Sequence
hGFAT1	72	Forward 5'-GCAAAGAGATCATGCTTGGA-3' Reverse 5'-TTTCGTCATCCATGCTCAGT-3'
hGFAT2	96	Forward 5'-AAGACACGGATGAAGAGGCT-3' Reverse 5'-GATAGCGCTTGCAATCAGAAG-3'
hGUS	81	Forward 5'-CTCATTGGAATTTGCGGATT-3' Reverse 5'-CCGAGTGAAGATCCCCTTTTA-3'
mGFAT1	114	Forward 5'-TGTTCTCGAACAAGACGAG-3' Reverse 5'-TCTTTGTCATGCTCCGT-3'
mGFAT2	86	Forward 5'-AAGCGCTCAGTACTGATGA-3' Reverse 5'-GCGCTGAAGTTACCTTTCATT-3'
mGUS	124	Forward 5'-AGGGCAGTGAACATTTCCAG-3'

Human (h) and mouse (m) GFAT1 and GFAT2 mRNA expression levels were determined by real-time PCR in parental and antisense GA expressing cell lines using the primers listed above.  $\beta$ -glucuronidase gene (GUS) was used as an internal control.

10,000g for 10 min and the supernatants saved until use.

In order to perform immunoprecipitation (IP), whole cell extracts were obtained by lysing the cells on ice with 1 ml of pre-cooled lysis buffer (150 mM NaCl, 50 mM Tris-HCl, pH 8.0, 1% Triton X-100 plus protease inhibitor cocktail) per 9 cm culture dish containing  $1-10 \times 10^6$  cells. The lysates were scrapped, transferred to a 1.5 ml tube and incubated for 30 min on ice with occasional mixing. The lysates were then centrifuged for 10 min at 10,000g at 4°C to eliminate cell debris. The supernatants were saved and stored at -20°C until IP.

#### Protein Immunoprecipitations

Whole cell lysates (500  $\mu$ g) were incubated with 50  $\mu$ l Protein A MicroBeads (Miltenyi Biotec, Germany) and 2  $\mu$ g of RL2 antibody or 10  $\mu$ g of  $\beta$ -catenin, Sp1, Rpt2, or TCP-1 antibodies. Lysates were incubated for 30 min on ice and later applied onto a  $\mu$ MACS column (Miltenyi Biotec). Proteins were eluted with 70  $\mu$ l of pre-heated (95°C) 1 $\times$  SDS-PAGE sample buffer. Heating of the buffer was necessary in order to facilitate protein desorption from the column. The eluted proteins were then ready for Western blotting.

#### Measurement of Sp1 Transcriptional Activity

The Sp1-dependent luciferase reporter plasmid pGAGC6 was a kind gift from Dr. Jeffrey Kudlow (School of Medicine, University of Alabama). The pGAGC6 plasmid contains six Sp1 consensus binding sites cloned into a luciferase reporter plasmid upstream of the adenovirus major late initiator TATA box. The plasmid pGAM, containing only the adenovirus TATA box, was used as a control. The plasmid

pCMV- $\beta$ -gal (containing the human cytomegalovirus promoter upstream of the  $\beta$ -galactosidase gene) was used to normalize luciferase activity.

Cotransfections of MCF7 and ORF19 cells with reporter and pCMV- $\beta$ -gal plasmids were carried out using Lipofectin Reagent (GibcoBRL) following the manufacturer's instructions. The combined detection of luciferase and  $\beta$ -galactosidase was performed with the Dual-Light System (Applied Biosystems). Expression of the luciferase enzymatic activity was normalized to  $\beta$ -galactosidase activity. Each transfection was repeated at least three times, and statistical differences were determined by using the U-Mann-Whitney test.

#### SDS-PAGE and Western Blotting Analysis

Whole cell extracts or eluted proteins were analyzed on a 10% SDS-PAGE and the electrophoresed proteins blotted onto nitrocellulose membranes (Protran, Schleicher & Schuell, Bioscience, Germany). The membranes were incubated with the primary antibody at the appropriate dilution for 2 h at room temperature.

After primary antibody incubation, the membranes were washed 4 $\times$  with TBS-Tween 20 and incubated with rabbit IgG True-blot (eBioscience, Boston, MA) to reveal immunoprecipitated  $\beta$ -catenin, Rpt2 or OGT, or with an appropriate secondary HRP-conjugated antibody to detect O-GlcNAc or TCP-1  $\theta$  proteins. Proteins were visualized by chemiluminescence using the ECL reagent (Amersham).

#### Two-Dimensional Gel Electrophoresis

O-glycosylated proteins from MCF7 and ORF19 cells were isolated using  $\mu$ MACS



columns and the RL2 antibody as described above. Proteins were eluted from the column with 125  $\mu$ l of lysis buffer (8.5 M urea, 2.2% (w/v) CHAPS, 0.5% (v/v) IPG buffer, bromophenol blue and DTT) and separated by 2D electrophoresis as follows. The first dimension was performed on a precast DryStrip IPG 3–10 L gel (linear immobilized pH 3–10 gradient gel), which was actively rehydrated overnight. The IPG gels were electrophoresed on a Bio-Rad Protean IEF cell unit under the following conditions: 250 V for 15 min and 4000 V for 120 min, and then run to accumulate a total of 10,000 V · h. The second dimension was run on a Mini protean II system (Bio-Rad) using 10% polyacrylamide gels in the presence of 0.1% (w/v) SDS. The 2D gels were stained with MALDI compatible Proteosilver<sup>TM</sup> Plus silver stain kit (Sigma). Duplicate 2D gels were run for every sample. Digitalized images of the gels were produced using a GS-800 calibrated densitometer (Bio-Rad) and the Quantity one software. Selected dots were cutted and mass spectrometry determinations were made with a Bruker MALDI-TOF/TOF Ultraflex equipment (Central Proteomics Facility, Universidad Autónoma de Barcelona, Spain).

## RESULTS

### Antisense Inhibition of LGA

MCF7 cells were transfected with a pcDNA3 plasmid containing the entire open reading frame of human L-type GA in the reverse orientation as described in the Materials and Methods Section. After transfection, 15 different cell clones were selected and their proliferation rates determined by cell enumeration using a Coulter counter. The MCF7 cell line and cell clones transfected with the pcDNA3 vector without any insert were used as controls. All clones transfected with the antisense LGA cDNA showed a decrease in the growth rate and glutaminase activity (Fig. 1A,B). There was a remarkable 50% inhibition of GA activity during the onset of the exponential growth phase. The diminished enzyme activity correlated with a lower expression of both LGA and KGA proteins, as assessed by Western blotting probed with isoform specific antibodies (see Fig. 1C). It is highly probable that due to a strong overall sequence similarity between LGA and KGA coding sequences, the antisense LGA mRNA transcript may inhibit both

isozymes. GA inhibition also reduced drastically the capacity of these cells to grow in a colony-forming assay (Fig. 1D) and forced tumor cell growth by cluster formation (Fig. 1E). The clone ORF19, showing a growth capacity almost 50% lower than control cells, was selected for further studies.

### Measurement of GFAT Activity and mRNA Levels in MCF7 and ORF19 Cells

GFAT activity was measured by quantitating the reaction product GlcN-6-P by HPLC. The activity was measured in MCF7 and ORF19 cells, as well as in the murine tumor cell EATC and its derivative 0.28AS-2 cells expressing a 280 bp segment of antisense mRNA coding for rat KGA [Lobo et al., 2000]. GFAT activity was threefold higher in the parental MCF7 and EATC tumor cell lines than in their antisense-expressing counterparts ORF19 and 0.28AS-2 cells (see Fig. 2). We then tried to evaluate GFAT mRNA abundance by real-time PCR in the parental and antisense expressing cells. Isoform specific primers were designed for the two isoforms of this enzyme, named GFAT1 and GFAT2. Nevertheless, isoform 2 could only be amplified in the positive control suggesting that GFAT2 is not expressed in the parental or antisense expressing cell lines. The real-time PCR results showed that GFAT1 expression was 40% lower in antisense mRNA expressing cells (Fig. 3).

### O-Glycosylation Status in Parental and Antisense GA Expressing Cell Lines

Since GFAT is the enzyme that controls the net flux through the hexosamine pathway, with this pathway providing UDP-GlcNAc as the substrate for the O-glycosylation of proteins, we next examined if the diminished GFAT activity could influence the net O-glycosylation status of cellular proteins in the antisense GA expressing cells. We tested the band pattern of O-glycosylated proteins by Western blot probed with the RL2 antibody, which is widely used for detecting O-GlcNAc modified proteins [Sayeski and Kudlow, 1996; Konrad et al., 2001]. As shown in Figure 4, no significant differences were observed in the global O-GlcNAc between the parental cells MCF7 and EATC and their counterpart ORF19 and 0.28AS-2 cells. However, because of the presence of some differentially expressed bands, we decided to look closer at the O-glycosylation status of key

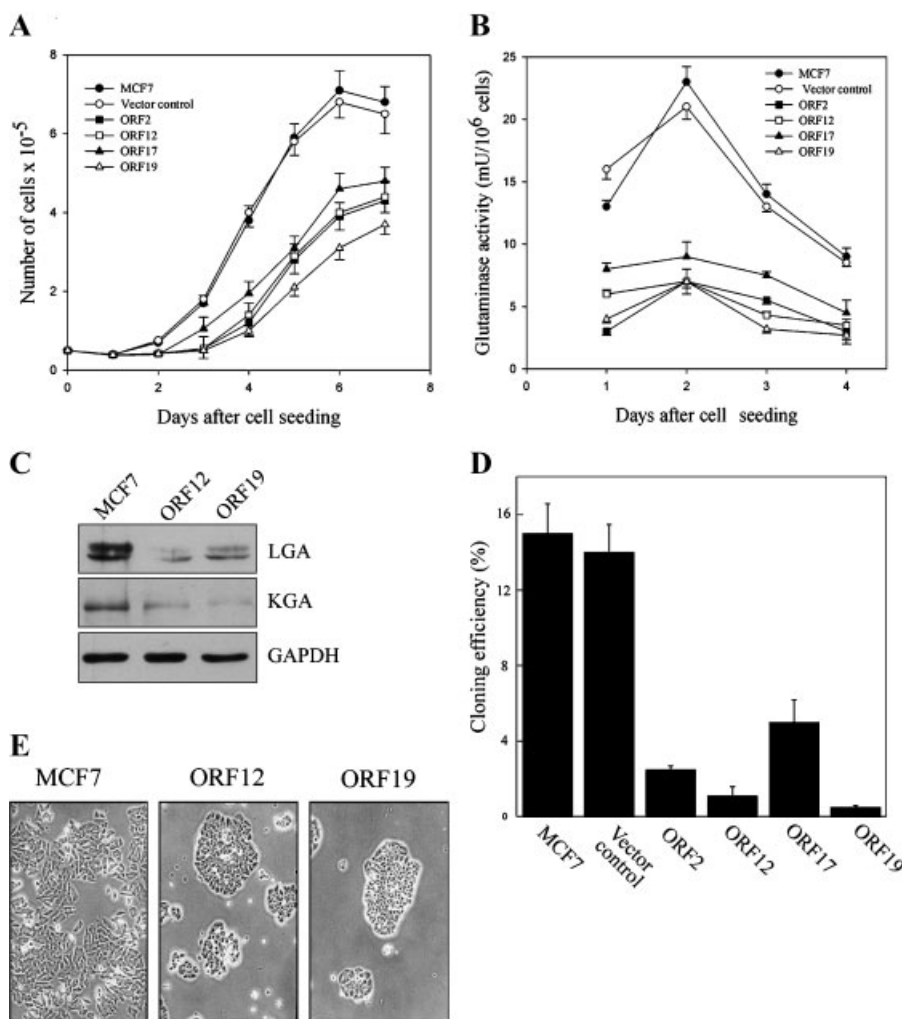


**Fig. 1.** Antisense inhibition of GA. MCF7 cells were transfected with a plasmid expressing the open reading frame of human L-type GA in antisense orientation. Parental and transfected cells (named ORF19) were characterized. **A:** Number of cells on different days after sub-culturing. **B:** GA activity. **C:** Western blotting of cellular extracts from MCF7 and ORF19 cells

harvested at day two after cell seeding. Protein detection was carried out with an isoform-specific anti-LGA (**upper panel**) or KGA (**lower panel**) antibody. **D:** Optical microscopy photograph of MCF7 and ORF19 cells. Both photographs are depicted at the same magnification. Values on **panels A,B** are represented as mean  $\pm$  SEM of at least three independent experiments.

tumor-relevant proteins in MCF7 and ORF19 cells. O-glycosylated proteins were immunoprecipitated by using the RL2 antibody, and detected by Western blotting with protein specific antibodies. Total protein content was determined by IP and detection with the same specific antibody. Then, we tested the O-glycosylation status of the enzyme OGT. This enzyme catalyzes the transfer of GlcNAc to proteins and can be also self-modified with O-GlcNAc. Figure 5A shows that although the total OGT content was slightly higher in ORF19 cells, the amount of O-glycosylated OGT was reduced fivefold in the ORF19 cells. It is known that O-glycosylation alters the protein function, but the role of this modification in OGT activity is

largely unknown. Presumably, it is involved in the protein-protein interaction processes and therefore it may alter the OGT substrate specificity [Wells et al., 2001]. We then studied the O-glycosylation status of  $\beta$ -catenin, a protein involved in the tumorigenic process of many tumors and known to be O-glycosylated [Morin, 1999; Kouzmenko et al., 2004]. In this case, we did not find any difference in the level of expression of O-glycosylated  $\beta$ -catenin between MCF7 and ORF19 cells (Fig. 5B).

#### Sp1 Expression, O-Glycosylation Pattern, and Transcriptional Activity

It has been established that O-glycosylation of Sp1 changes its transcriptional activity

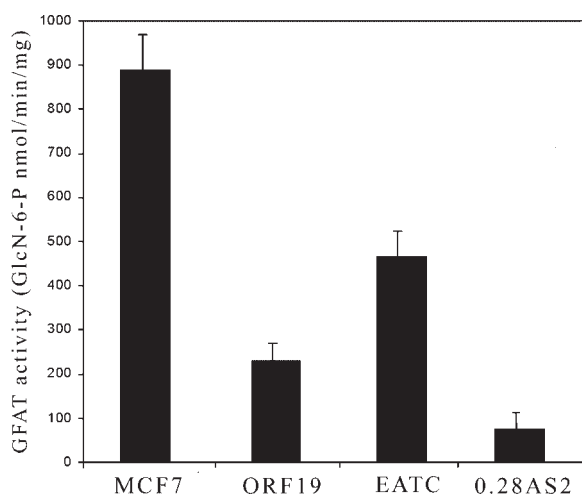


**Fig. 2.** GFAT activity measurement. Cellular extracts from parental and antisense GA expressing cells harvested at the exponential phase of growth were prepared as described in the Materials and Methods Section. GFAT activity was measured by quantification of the reaction product GlcN-6-P by HPLC and represented as the mean  $\pm$  SEM of at least three independent experiments.

[Wells et al., 2001], and glutamine has been involved in this mechanism [Brasse-Lagnel et al., 2003]. In addition, an enhanced Sp1 transcriptional activity has previously been reported in the 0.28AS-2 antisense GA expressing cells [Segura et al., 2005]. For these reasons, we investigated the effect of antisense GA inhibition on Sp1 in MCF7 and ORF19 cells. Whilst the relative abundance of Sp1 was 10-fold

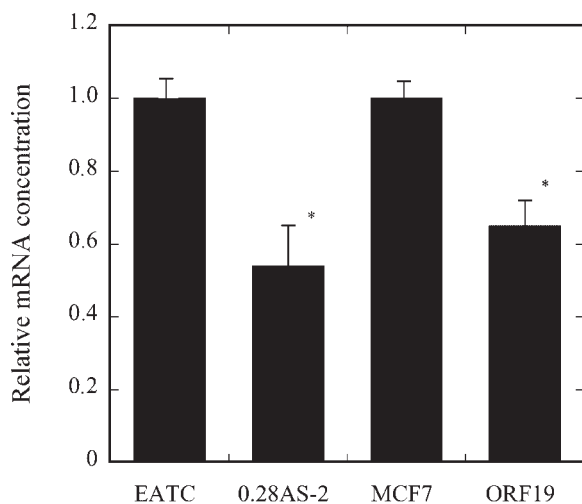


**Fig. 3.** Real-time PCR quantification of GFAT mRNA. Total RNA from the wild type and antisense GA expressing cell lines was isolated and analyzed by RT-PCR. GFAT expression was normalized to  $\beta$ -glucuronidase mRNA and is presented relative to wild type control cell lines. \*Denotes significant difference ( $P < 0.05$ ) from the untreated control.

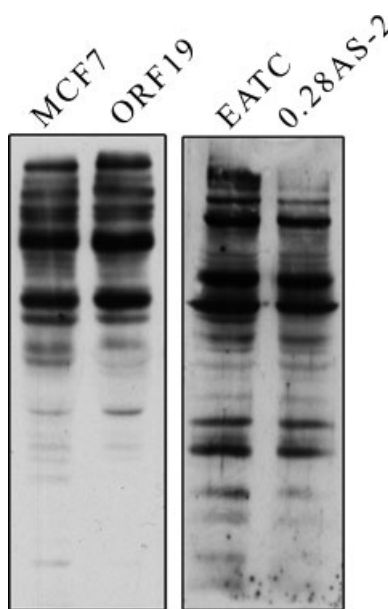


**Fig. 4.** Total O-GlcNAc protein content. Cellular extracts from parental and antisense GA mRNA expressing cells were harvested at the exponential growth phase and submitted to Western blotting using the RL2 antibody that specifically recognizes O-GlcNAc residues in proteins.

higher in ORF19 than in wild type MCF7 cells, the amount of O-GlcNAc-Sp1 only showed a threefold increase (Fig. 5C). This indicates that although the Sp1 expression was higher in ORF19 cells, its degree of O-glycosylation was smaller. The Sp1 transcriptional activity was also measured in MCF7 and ORF19 cells using the pGAGC6 plasmid, which contains six Sp1 consensus-binding sites. The plasmid pGAM, containing only the adenovirus TATA box, was used as a control. The results (Table II) clearly showed a significant increase (up to sixfold) of the Sp1 transcriptional activity in ORF19 cells.

Since O-glycosylation of the Rpt2 component of the proteasome is greatly responsible for Sp1 degradation, we also studied the O-glycosylation status of Rpt2 protein in MCF7 and ORF19 cells. We detected a fourfold increase in the total Rpt2 expression in ORF19 cells (Fig. 5D). However, the O-glycosylated Rpt2 form only increased 1.5-fold. Thus, in a similar fashion to that occurring to Sp1, Rpt2 expression was higher in ORF19 cells, although its O-glycosylation degree was smaller.

#### Identification of Differentially Expressed O-Glycosylated Proteins by Proteomic Analysis

In order to identify proteins that were differentially modified by O-glycosylation due to

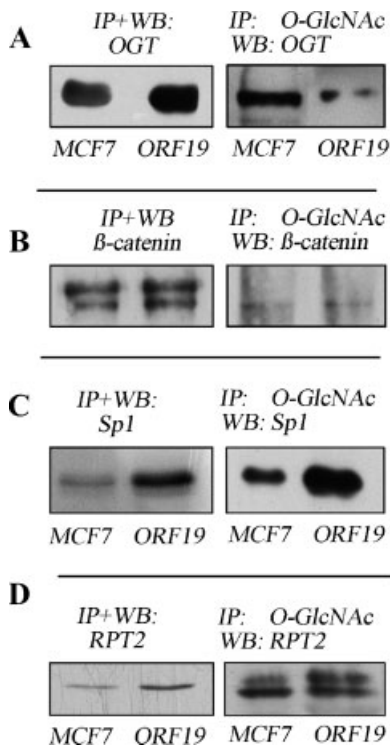


**Fig. 5.** Determination of the O-GlcNAc pattern in relevant proteins. Cellular extracts of parental and antisense GA mRNA expressing cells were harvested at the exponential phase of growth. Total protein content of (A) OGT, (B)  $\beta$ -catenin, (C) Sp1, and (D) Rpt2, were determined by IP using specific primary antibodies followed by Western blotting with the same antibody. We carried out the quantification of O-glycosylated proteins by IP with RL2 antibody followed by Western blots using the specific primary antibody.

antisense inhibition of GA, we designed a protocol based on the IP of total O-glycosylated proteins using the RL2 antibody, followed by their separation using 2D gel electrophoresis and mass spectrometry identification of the differentially O-GlcNAc proteins. Two 2D gels

**TABLE II. Measurement of Sp1 Transcriptional Activity**

Plasmid	Specific activity (RLU/mg protein)	
	MCF7	ORF19
pGAM	0.44 ± 0.03	0.72 ± 0.08
pGAGC6	9.22 ± 0.85	113.59 ± 15.20

MCF7 and ORF19 cells were transfected with pGAGC6 luciferase reporter plasmid containing six consecutive Sp1 consensus sequences upstream of the adenovirus major late initiator TATA box. The plasmid pGAM, containing only the adenovirus TATA box, was used as a control. Luciferase activity is shown as relative luciferase units (RLU)/mg protein. Each data represents the average ± SD for three independent experiments.

were run in parallel, in order to analyze IP obtained from MCF7 and ORF19 cells. After silver staining and comparison of spot distribution using PDQuest software, candidate spots were analyzed by MALDI-TOF. Typical 2D gels are shown in Figure 6A,B. Several differentially expressed protein spots were chosen for analysis. Two clear positives were unambiguously identified after mass spectrometry analysis, one corresponding to the human T-complex protein 1, theta subunit (TCP-1- $\theta$ , UniProtKB accession

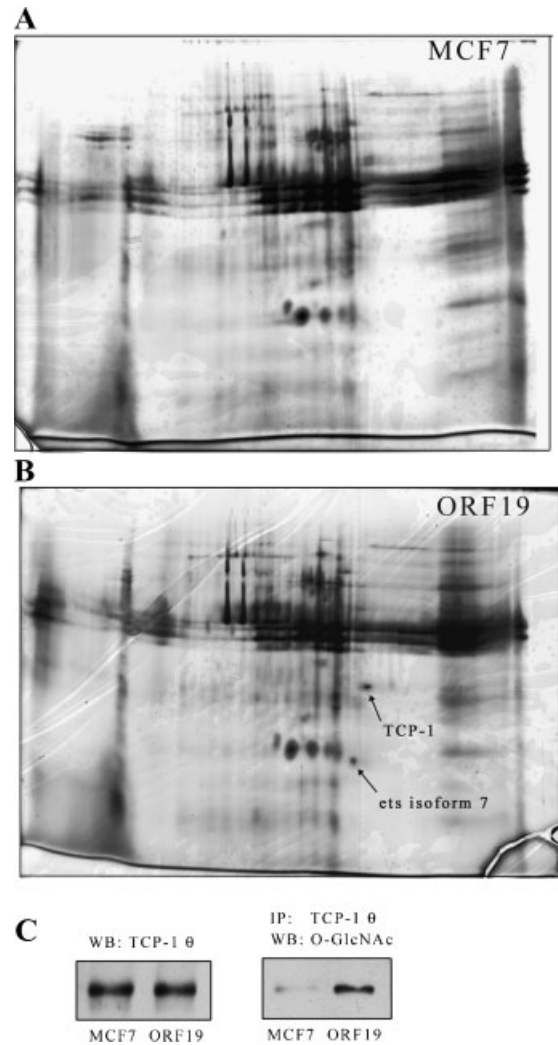


**Fig. 6.** Two-dimensional gel electrophoresis. Cellular protein extracts from MCF7 (panel A) and ORF19 (panel B) harvested at the exponential phase of growth were separated by 2D gel electrophoresis as described in the Materials and Methods Section. Differentially expressed O-glycosylated proteins were analyzed by mass spectrometry (MALDI-TOF). The O-glycosylation status of TCP-1  $\theta$  was confirmed by IP using anti-TCP-1  $\theta$  antibody followed by Western blot using the RL2 antibody (panel C, right). The total amount of TCP-1  $\theta$  was revealed using anti-TCP-1  $\theta$  as a secondary antibody (panel C, left).



# P50990), and the other to the human Ets-related protein isoform 7 (UniProtKB accession # Q6XXX5). To further confirm O-GlcNAc modification of TCP-1- $\theta$ , we carried out IP of TCP-1- $\theta$  using specific antibodies, followed by Western blotting with RL2 antibody. Figure 6C shows that immunoprecipitated TCP-1- $\theta$  could be recognized by the RL2 antibody that specifically binds O-GlcNAc residues in proteins. Furthermore, an increase in the O-glycosylated TCP-1- $\theta$  form in ORF19 cells was also confirmed, while the total TCP-1- $\theta$  protein level remained constant. The lack of commercially available antibodies against the human Ets protein prevented us from being able to check its O-glycosylated status by Western analysis.

## DISCUSSION

In the present work, we have studied the effects of tumor GA inhibition on the hexosamine pathway, a metabolic route that functions as a nutrient sensor. This route serves as a source of UDP-GlcNAc, the substrate for O-glycosylation of proteins.

In tumor cells, GA is over-expressed and it hydrolyzes glutamine at high rates, yielding glutamate and ammonium ions. Glutamate can be further metabolized by a partial oxidation producing aspartate. However the major part of the glutamine yields glutamate, which is mostly excreted as an end product [Souba, 1993]. This apparent wasteful consumption of glutamine could be justified if the rapid hydrolysis of glutamine is connected to the indirect energetization of amino acid transport [Aledo, 2004]. The importance of maintaining a high GA activity in tumor cells is indeed demonstrated by the profound effects caused by GA inhibition in rapidly dividing cells, generating a deficit in the cellular energy and nitrogen supplies that drives the cells to dramatically change their phenotype and tumorigenicity [Lobo et al., 2000; Segura et al., 2001]. Since a first consequence of GA inhibition is an increase in the intracellular glutamine concentration [Márquez and Núñez de Castro, 1991; Lora et al., 2004], the *in vivo* activity of enzymes that use glutamine as a substrate, such as GFAT, could be affected. This change in intracellular glutamine concentration could also affect glutamine-utilizing enzymes through other mechanisms involving glutamine sensing and signaling. The finding that the mRNA GFAT

level is not greatly changed points towards allosteric modulation or post-translational modifications of the enzyme as responsible for GFAT inhibition in antisense GA expressing cells. Mechanisms exist to reduce GFAT activity, such as phosphorylation by cAMP-dependent protein kinase A [Chang et al., 2000] or allosteric inhibition by UDP-GlcNAc, the strongest natural inhibitor of GFAT with an  $IC_{50}$  value of 7  $\mu$ M [Broschat et al., 2002].

Determining how this reduced GFAT activity could affect O-GlcNAc protein modification was our next goal. We showed that OGT itself, the enzyme that carries out the transfer of O-GlcNAc to proteins, had a fivefold lower O-glycosylation level in ORF19 cells than in MCF7 cells. OGT contains an N-terminal protein interaction domain, consisting of multiple tetratricopeptide repeats that control the enzyme's affinity for targeting proteins. However, other post-translational modifications, such as phosphorylation and O-glycosylation, greatly increase the complexity of OGT regulation. Although these post-translational modifications have not been mapped out, with it being largely unknown how they affect its enzymatic activity [Slawson et al., 2006], it is tempting to speculate that the reduced levels of O-glycosylated OGT may affect its target selection, since total O-glycosylated proteins and total OGT protein did not significantly change in ORF19 cells.

O-GlcNAc plays a central role in the regulation of gene transcription. Many transcription factors, and also RNA polymerase II itself, are modified by O-GlcNAc [Wells et al., 2001]. One of the OGT targets is Sp1, where O-glycosylation plays an important role in regulating its transcriptional activity [Jackson and Tjian, 1988]. Our results show a 10-fold increase in total Sp1 protein together with a threefold reduction of the O-glycosylation degree of Sp1 as a consequence of GA inhibition. In this regard, it is important to remark that O-glycosylation affects Sp1 stability through inhibition of the ATPase activity of the Rpt2 proteasome component [Zhang et al., 2003]. Since we have observed a significant decrease in the ratio of O-glycosylated to total Rpt2 in ORF19 cells, this fact could explain the higher Sp1 content in these cells. Nevertheless, additional work is needed to test this hypothesis.

We have shown that inhibition of GA leads to an increase in Sp1 transcriptional activity in

ORF19 cells (Table II), with this being also reproduced in murine EATC cells expressing antisense GA mRNA [Segura et al., 2005]. This fact could be explained as a consequence of both the increased Sp1 protein content and the reduced O-GlcNAc-Sp1/total Sp1 ratio. It is well known that O-linkage of GlcNAc to Sp1 activation domain inhibits its transcriptional capability [Yang et al., 2001].

Proteome analysis of O-GlcNAc proteins enabled us to detect two new OGT target proteins: TCP-1  $\theta$  and human Ets-related protein isoform 7. Both proteins are over glycosylated in ORF19 cells, reinforcing the notion that a reduction of O-glycosylated OGT does not imply a net reduction of the O-glycosylated proteins. TCP-1  $\theta$  is a subunit of the hetero-oligomeric complex CCT (chaperonin containing TCP-1) present in the eukaryotic cytosol. TCP is composed of eight different subunit species that are proposed to have independent functions in folding their *in vivo* substrates: actin and tubulin (for a review see [Frydman, 2001]). TCP-1  $\theta$  has not been previously described to be O-glycosylated. Therefore, we confirmed the result by IP of TCP-1  $\theta$  and further detection with the RL2 antibody. Also, we can speculate that O-glycosylation of TCP-1  $\theta$  affects actin and tubulin folding in a way that favors the acquisition of a more differentiated phenotype in ORF19 cells. Human Ets-related protein isoform 7, on the other hand, belongs to the ERG (Ets-related gene) family. ERG may participate in transcriptional regulation through the recruitment of SETDB1 histone methyltransferase and subsequent modification of the local chromatin structure [Murakami et al., 1993]. The ERG transcription factor has been implicated as a key mediator in the process of angiogenesis, and also plays a role in a large number of diseases, including cancer and inflammatory conditions such as rheumatoid arthritis [McLaughlin et al., 2001]. In cancer, ERG behaves as an oncogene, and is involved in Ewing sarcoma and acute myeloid leukemia [Delattre et al., 1994].

In summary, the inhibition of GA expression makes tumors unable to consume glutamine at high rates, depriving the cells of an important source of energy and nitrogen and forcing cancer cells to be less proliferative and to acquire a more differentiated phenotype. We have shown that the reduction of the

hexosamine pathway and the changes in O-GlcNAc target proteins are also remarkable aspects of GA inhibition. The adaptation of the cell to the new nutritional and energetic status can be partially mediated by regulating the targeting of O-GlcNAc to the key proteins controlling cell proliferation and differentiation, such as OGT, Sp1, Rpt2, TCP-1  $\theta$ , and ERG.

#### ACKNOWLEDGMENTS

The present work has been supported by a grant from the Plan Nacional de Investigación y Desarrollo (SAF 2004-02339) of the Ministry of Education and Science of Spain. M.M.-R. is a fellow of a Consortium funded by the private company HUTESA, S.A. (Fuente de Piedra, Málaga, Spain) and sponsored by the Confederación de Empresarios de Málaga (CEM) and the Foundation of the University of Málaga. A.C.D. was a recipient of a project from AECEI, program Intercampus. C.L. was contracted by Grant SAF2004-02339 as a Research Specialist. We thank Dr. Paul Hobson, native speaker, for revision of the manuscript.

#### REFERENCES

- Aledo JC. 2004. Glutamine breakdown in rapidly dividing cells: Waste or investment? *Bioessays* 26:778–785.
- Aledo JC, Gómez-Fabre PM, Olalla L, Márquez J. 2000. Identification of two human glutaminase loci and tissue-specific expression of the two related genes. *Mamm Genome* 11:1107–1110.
- Brasse-Lagnel C, Fairand A, Lavoine A, Husson A. 2003. Glutamine stimulates argininosuccinate synthetase gene expression through cytosolic O-glycosylation of Sp1 in Caco-2 cells. *J Biol Chem* 278:52504–52510.
- Broschat KO, Gorka C, Page JD, Martin-Berger CL, Davies MS, Huang Hc HC, Gulve EA, Salsgiver WJ, Kasten TP. 2002. Kinetic characterization of human glutamine-fructose-6-phosphate amidotransferase I: Potent feedback inhibition by glucosamine 6-phosphate. *J Biol Chem* 277:14764–14770.
- Chang Q, Su K, Baker JR, Yang X, Paterson AJ, Kudlow JE. 2000. Phosphorylation of human glutamine:fructose-6-phosphate amidotransferase by cAMP-dependent protein kinase at serine 205 blocks the enzyme activity. *J Biol Chem* 275:21981–21987.
- Curthoys NP, Watford M. 1995. Regulation of glutaminase activity and glutamine metabolism. *Annu Rev Nutr* 15: 133–159.
- Daniels MC, Ciaraldi TP, Nikoulina S, Henry RR, McClain DA. 1996. Glutamine:fructose-6-phosphate amidotransferase activity in cultured human skeletal muscle cells: Relationship to glucose disposal rate in control and non-insulin-dependent diabetes mellitus subjects

- and regulation by glucose and insulin. *J Clin Invest* 97: 1235–1241.
- Delattre O, Zucman J, Melot T, Garau XS, Zucker JM, Lenoir GM, Ambros PF, Sheer D, Turc-Carel C, Triche TJ, et al. 1994. The Ewing family of tumors—a subgroup of small-round-cell tumors defined by specific chimeric transcripts. *N Engl J Med* 331:294–299.
- Elgadi KM, Meguid RA, Qian M, Souba WW, Abcouwer SF. 1999. Cloning and analysis of unique human glutaminase isoforms generated by tissue-specific alternative splicing. *Physiol Genomics* 1:51–62.
- Frydman J. 2001. Folding of newly translated proteins in vivo: The role of molecular chaperones. *Annu Rev Biochem* 70:603–647.
- Gómez-Fabre PM, Aledo JC, Castillo-Olivares A, Alonso FJ, Núñez de Castro I, Campos JA, Márquez J. 2000. Molecular cloning, sequencing and expression studies of the human breast cancer cell glutaminase. *Biochem J* 345:365–375.
- Heini HG, Gebhardt R, Brecht A, Mecke D. 1987. Purification and characterization of rat liver glutaminase. *Eur J Biochem* 162:541–546.
- Holt GD, Hart GW. 1986. The subcellular distribution of terminal N-acetylglucosamine moieties. Localization of a novel protein-saccharide linkage, O-linked GlcNAc. *J Biol Chem* 261:8049–8057.
- Jackson SP, Tjian R. 1988. O-glycosylation of eukaryotic transcription factors: Implications for mechanisms of transcriptional regulation. *Cell* 55:125–133.
- Ko YG, Kim EY, Kim T, Park H, Park HS, Choi EJ, Kim S. 2001. Glutamine-dependent antiapoptotic interaction of human glutaminyl-tRNA synthetase with apoptosis signal-regulating kinase 1. *J Biol Chem* 276:6030–6036.
- Konrad RJ, Mikolaenko I, Tolar JF, Liu K, Kudlow JE. 2001. The potential mechanism of the diabetogenic action of streptozotocin: Inhibition of pancreatic beta-cell O-GlcNAc-selective N-acetyl-beta-D-glucosaminidase. *Biochem J* 356:31–41.
- Kouzmenko AP, Takeyama K, Ito S, Furutani T, Sawatsubashi S, Maki A, Suzuki E, Kawasaki Y, Akiyama T, Tabata T, Kato S. 2004. Wnt/beta-catenin and estrogen signaling converge in vivo. *J Biol Chem* 279:40255–40258.
- Lobo C, Ruía-Bellido MA, Aledo JC, Márquez J, Núñez de Castro I, Alonso FJ. 2000. Inhibition of glutaminase expression by antisense mRNA decreases growth and tumorigenicity of tumor cells. *Biochem J* 348:257–261.
- Lora J, Alonso FJ, Segura JA, Lobo C, Márquez J, Matés JM. 2004. Antisense glutaminase inhibition decreases glutathione antioxidant capacity and increases apoptosis in Ehrlich ascitic tumour cells. *Eur J Biochem* 271:4298–4306.
- Márquez J, Núñez de Castro I. 1991. Mouse liver free amino acids during the development of Ehrlich ascites tumour. *Cancer Lett* 58:221–224.
- Márquez J, de la Oliva AR, Matés JM, Segura JA, Alonso FJ. 2006. Glutaminase: A multifaceted protein not only involved in generating glutamate. *Neurochem Int* 48: 465–471.
- Matés JM, Segura JA, Alonso FJ, Márquez J. 2006. Pathways from glutamine to apoptosis. *Front Biosci* 11: 3164–3180.
- McLaughlin F, Ludbrook VJ, Cox J, von Carlowitz I, Brown S, Randi AM. 2001. Combined genomic and antisense analysis reveals that the transcription factor Erg is implicated in endothelial cell differentiation. *Blood* 98: 3332–3339.
- Medina MA, Sánchez Jiménez F, Márquez J, Rodríguez Quesada A, Nuñez de Castro I. 1992. Relevance of glutamine metabolism to tumor cell growth. *Mol Cell Biochem* 113:1–15.
- Morin PJ. 1999. Beta-catenin signaling and cancer. *Bioessays* 21:1021–1030.
- Murakami K, Mavrothalassitis G, Bhat NK, Fisher RJ, Papas TS. 1993. Human ERG-2 protein is a phosphorylated DNA-binding protein—a distinct member of the ets family. *Oncogene* 8:1559–1566.
- Nakajo T, Yamatsuji T, Ban H, Shigemitsu K, Haisa M, Motoki T, Noma K, Nobuhisa T, Matsuoka J, Gunduz M, Yonezawa K, Tanaka N, Naomoto Y. 2005. Glutamine is a key regulator for amino acid-controlled cell growth through the mTOR signaling pathway in rat intestinal epithelial cells. *Biochem Biophys Res Commun* 326: 174–180.
- Olalla L, Gutiérrez A, Campos JA, Khan ZU, Alonso FJ, Segura JA, Márquez J, Aledo JC. 2002. Nuclear localization of L-type glutaminase in mammalian brain. *J Biol Chem* 277:38939–38944.
- Pérez-Gómez C, Campos-Sandoval JA, Alonso FJ, Segura JA, Manzanares E, Ruíz-Sánchez P, González ME, Márquez J, Matés JM. 2005. Co-expression of glutaminase K and L isoenzymes in human tumour cells. *Biochem J* 386:535–542.
- Rhoads JM, Argenzio RA, Chen W, Rippe RA, Westwick JK, Cox AD, Berschneider HM, Brenner DA. 1997. L-glutamine stimulates intestinal cell proliferation and activates mitogen-activated protein kinases. *Am J Physiol* 272:G943–953.
- Sayeski PP, Kudlow JE. 1996. Glucose metabolism to glucosamine is necessary for glucose stimulation of transforming growth factor- $\alpha$  gene transcription. *J Biol Chem* 271:15237–15243.
- Segura JA, Ruíz-Bellido MA, Arenas M, Lobo C, Márquez J, Alonso FJ. 2001. Ehrlich ascites tumor cells expressing anti-sense glutaminase mRNA lose their capacity to evade the mouse immune system. *Int J Cancer* 91:379–384.
- Segura JA, Donadio AC, Lobo C, Mates JM, Márquez J, Alonso FJ. 2005. Inhibition of glutaminase expression increases Sp1 phosphorylation and Sp1/Sp3 transcriptional activity in Ehrlich tumor cells. *Cancer Lett* 218: 91–98.
- Slawson C, Housley MP, Hart GW. 2006. O-GlcNAc cycling: How a single sugar post-translational modification is changing the way we think about signaling networks. *J Cell Biochem* 97:71–83.
- Smith EM, Watford M. 1990. Molecular cloning of a cDNA for rat hepatic glutaminase. Sequence similarity to kidney-type glutaminase. *J Biol Chem* 265:10631–10636.
- Souba WW. 1993. Glutamine and cancer. *Ann Surg* 218: 715–728.
- Tapiero H, Mathe G, Couvreur P, Tew KD. 2002. II. Glutamine and glutamate. *Biomed Pharmacother* 56: 446–457.
- Torres CR, Hart GW. 1984. Topography and polypeptide distribution of terminal N-acetylglucosamine residues on the surfaces of intact lymphocytes. Evidence for O-linked GlcNAc. *J Biol Chem* 259:3308–3317.

- Turner A, McGivan JD. 2003. Glutaminase isoform expression in cell lines derived from human colorectal adenomas and carcinomas. *Biochem J* 370:403–408.
- Tzagarakis-Foster C, Geleziunas R, Lomri A, An J, Leitman DC. 2002. Estradiol represses human T-cell leukemia virus type 1 Tax activation of tumor necrosis factor- $\alpha$  gene transcription. *J Biol Chem* 277:44772–44777.
- Wells L, Vosseller K, Hart GW. 2001. Glycosylation of nucleocytoplasmic proteins: Signal transduction and O-GlcNAc. *Science* 291:2376–2378.
- Yang X, Su K, Roos MD, Chang Q, Paterson AJ, Kudlow JE. 2001. O-linkage of N-acetylglucosamine to Sp1 activation domain inhibits its transcriptional capability. *Proc Natl Acad Sci U S A* 98:6611–6616.
- Zachara NE, Hart GW. 2004. O-GlcNAc a sensor of cellular state: The role of nucleocytoplasmic glycosylation in modulating cellular function in response to nutrition and stress. *Biochim Biophys Acta* 1673:13–28.
- Zhang F, Su K, Yang X, Bowe DB, Paterson AJ, Kudlow JE. 2003. O-GlcNAc modification is an endogenous inhibitor of the proteasome. *Cell* 115:715–725.